Plant Archives Vol. 20 Supplement 1, 2020 pp. 705-714 **e-ISSN:2581-6063 (online), ISSN:0972-5210**

SPATIAL SOIL EROSION RISK ASSESSMENT USING CORINE MODEL : A CASE STUDY IN WADI EL-RAML WATERSHED, NORTH WESTERN COAST, EGYPT

Ibraheem A. H. Yousif[1*], Essam el dine M. A. Tealab[1], Ali A. Abdel Hady[1] and Abdalsamad A. A. Aldabaa[2]

[1]Department of Soil Science, Faculty of Agriculture, Cairo University, Giza, 12613, Egypt.
[2]Department of Pedology, Water resources and Desert Soils Division, Desert Research Center, Egypt.

Abstract

Soil erosion is an important factor threaten the agricultural development in the northwestern coast of Egypt. Land cover, slope, soil erodibility and climate are the main factors affecting the quantity and severity of soil erosion. The main objective of this study was to estimate and assess actual (ASER) and potential soil erosion risk (PSER) of Wadi El-Raml basin using the CORINE model with RS and GIS. DEM was used to extract watershed, sub-watershed and slope gradients maps of the studied area. Landsat OLI image was used to generate land cover in ENVI 5.1. Fifty-four soil profiles were dug to represent all sub-watersheds. The digital maps of the soil texture, soil depth, stoniness and slope were generated in ArcGIS 10.3 and then inserted as CORINE inputs to create the PSER and ASER maps. The results indicated that 27.75%, 50.37% and 21.88% of the investigated area were under low, moderate and high actual soil erosion risk, respectively. It can be concluded that the methodology of CORINE model incorporated with GIS and RS has very effective and accurate potential for soil erosion risk assessment in the wide watersheds in the northwestern coast of Egypt.

Key words : Soil erosion, CORINE model, GIS, RS, Egypt.

Introduction

Soil erosion is the most important factor which damages and decreases the productivity of our agricultural soils, one of the most essential natural resources (Shpkinah and Saraswathy, 2005; Edosomwan *et al*., 2013). Furthermore, Soil erosion is a critical problem throughout the world due to its counteractive economic and ecological impacts such as losses in land and reduces in its productivity (Eroglu *et al*., 2010; El-Nady and Shoman, 2017). Therefore, estimation of soil erosion risk is necessary to conserve our agricultural lands and to achieve the sustainable management of watersheds. The Rainfall and runoff data analysis is requisite for crop planning and also help to characterize the extent of soil erosion, in addition to be helpful for water harvesting and reuse on watershed basis (Aahikari *et al*., 2004). There are many factors effect on the soil erosion such as soil erodibility, slope, texture, vegetation, organic matter, parent material and rainfall (Omuto and Vargas, 2009; Jakhar *et al*., 2012). Assessment of soil erosion using classical methods is time-consuming and expensive (Lakkad *et al*., 2018), therefore models providing assumption for forthcoming cases are very crucial. During the previous decades numerous models of soil erosion prediction have been proposed and developed, Universal Soil Loss Equation (USLE), ICONA (Institute for the Conservation of the Nature), Erosion Kinematic Wave Models, Discrete Dynamic Models (DDM) and the coordination of information on the environment (CORINE model) (Aksoy and Kavvas, 2005; De Vente *et al*., 2005; Cilek *et al*., 2015). These empirical models play a strong role in environmental risk assessment across the world because of their simple structure and ease of application (Ýmamoglu *et al*., 2014). CORINE is an empirical and

***Author for correspondence :** E-mail : ibraheemyousif@agr.cu.edu.eg

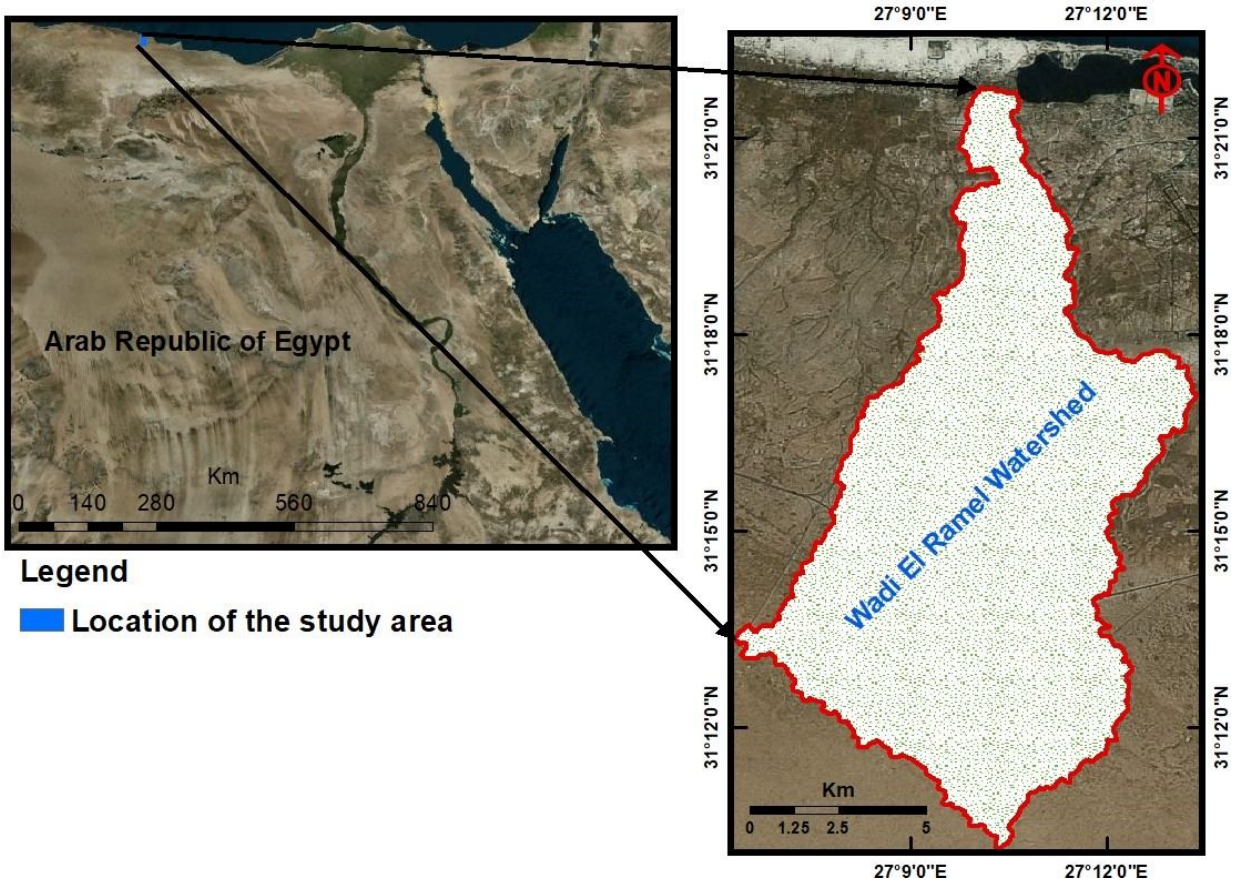

Fig. 1 : Location map of study area.

cartographic technique that includes overlaying of some layers to show the spatial heterogeneity of soil erosion risk (SER) within Arc-GIS environment (CORINE, 1992). The CORINE model was widely applied by the many researchers to assess the SER in different regions (Husnjak *et al*., 2008; Aydýn and Tecimen, 2010). GIS and remote sensing (RS) technologies are powerful tools in environmental assessment through its advance features for manipulating and analyzing spatial data (Singh *et al*., 2007; Yuksel *et al*., 2008; Yousif and Ahmed, 2019). Therefore, in the present study, an attempt of integration between GIS, RS, and CORINE model has been made to estimate soil erosion risk at Wadi El-Raml watershed using CORINE Model and GIS.

Materials and Methods

Study area

Wadi El-Raml watershed is located at west of Matrouh City, north western coast of Egypt between 27^0 04' 27.21" - 27^0 12' 29.98" E as longitudes and 31^0 09' 20.09" - 31^0 21' 57.87" N as latitudes (fig. 1) covering an area of 106.98 km^2. The mean annual temperature varied from 14.99 to 26.62^{o}C and the annual rainfall varied between 111.60 and 201.65 mm (E.M.A., 2018). The studied soils are characterized by torric moisture and hyperthermic temperature regimes (Soil Survey Staff, 2014). The investigated area dominated by a sedimentary succession varied from Middle Miocene to Quaternary (El-Shazely *et al*., 1975) as shown in fig. 2.

Soil sampling

Using hydrological modeling in ArcGIS, digital elevation model (DEM) with 30 m spatial resolution (fig. 3) was used to derive some parameters such as flow direction, flow accumulation, basins and sub-basins (ESRI, 2012). Fifty-four soil profiles were dug randomly to represent all sub-basins of the study area (Figure 4). Soil samples were collected and prepared for laboratory work. Soil physical and chemical analysis were done according to USDA (2014). Then soils were classified according to Soil Survey Staff (2014).

CORINE model

In CORINE model, four indices indulging erodibility, erosivity, slope and land cover were utilized to estimate the PSER and actual soil erosion risk (ASER). These data were processed through the map algebra in the Arc-GIS and allowed obtaining maps potential and current erosion indices, according to the methodology illustrated

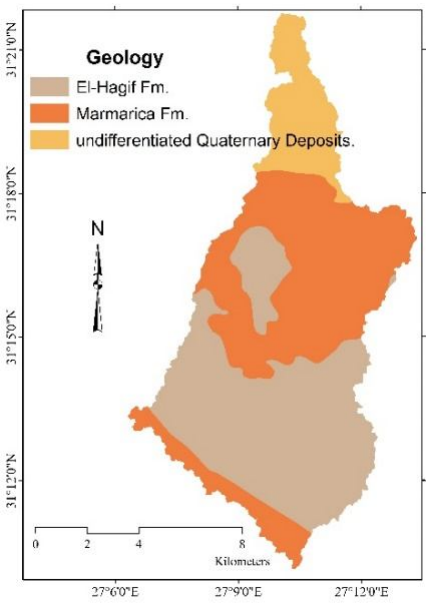

Fig. 2 : Geological map of the studied area.

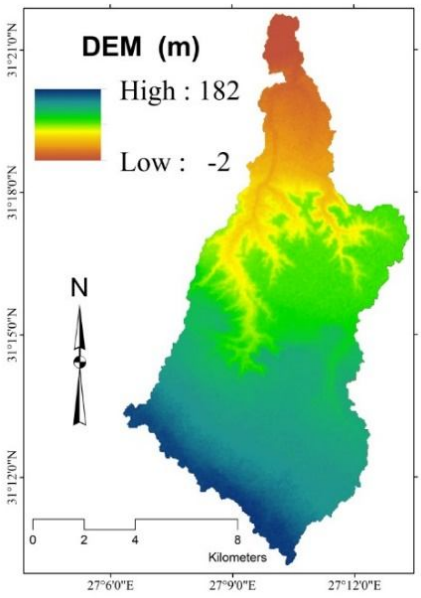

Fig. 3 : Digital Elevation Model of the studied area.

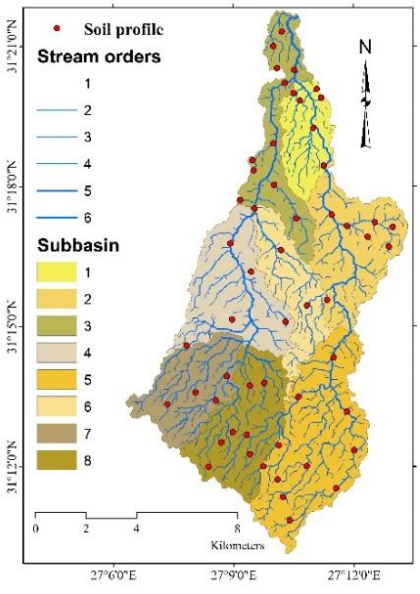

Fig. 4 : Soil profiels distribution in the studied area.

Table 1 : Classes and ranking of the various parameters used for assessment of soil erodibility (Aydin and Tecimen, 2010).

Soil parameter	Class	Index	Description
Soil Texture	Clay-Sandy Clay- Silty Clay	1	Slightly erodible
	Sandy Clay Loam - Clay Loam-Silty Clay Loam –Loamy Sand - Sandy	2	Moderately erodible
	Loam -Silty Loam – Silty - Sandy Loam	3	Highly erodible
Stoniness (%)	< 10	1	Not fully protected
	> 10	2	Fully protected
Soil Depth (cm)	> 75	1	Slightly erodible
	25-75	2	Moderately erodible
	< 25	3	Highly erodible
Erodibility	0-3	1	Low Erodibility
	3-6	2	Moderate Erodibility
	>6	3	High Erodibility

in fig. 5.

Soil erodibility

Soil erodibility is calculated as the product of these three indices, as following (CORINE, 1992): Index of soil erodibility = soil texture × soil depth × percentage of stones covered.

The erodibility map was created using Spatial Analyst extension (Map algebra) of ArcGIS 10.3 then indices were reclassified as presented in table 1.

Rainfall erosion index (Erosivity Index)

Erosivity index was calculated based on the rainfall and temperature data (table 2) of the Matrouh metrological station (2000 – 2018) and calculated as following.

Rainfall erosion index = Fournier (FI) index × Bagnold-Gawsn (BGI) index

$$\text{The Fournier index (FI)} = \sum_{i=1}^{12} \frac{P_i^2}{P} \text{ (Yuksel } et\ al.\text{, 2008)}$$

Where, p_i: the monthly precipitation (mm).

p : Total annual rainfall (mm).

$$\text{The Bagnold} - \text{Gawsn Index (BGI)} = \sum_{i=1}^{12} \left(2t_1 - p_1\right) k_1$$

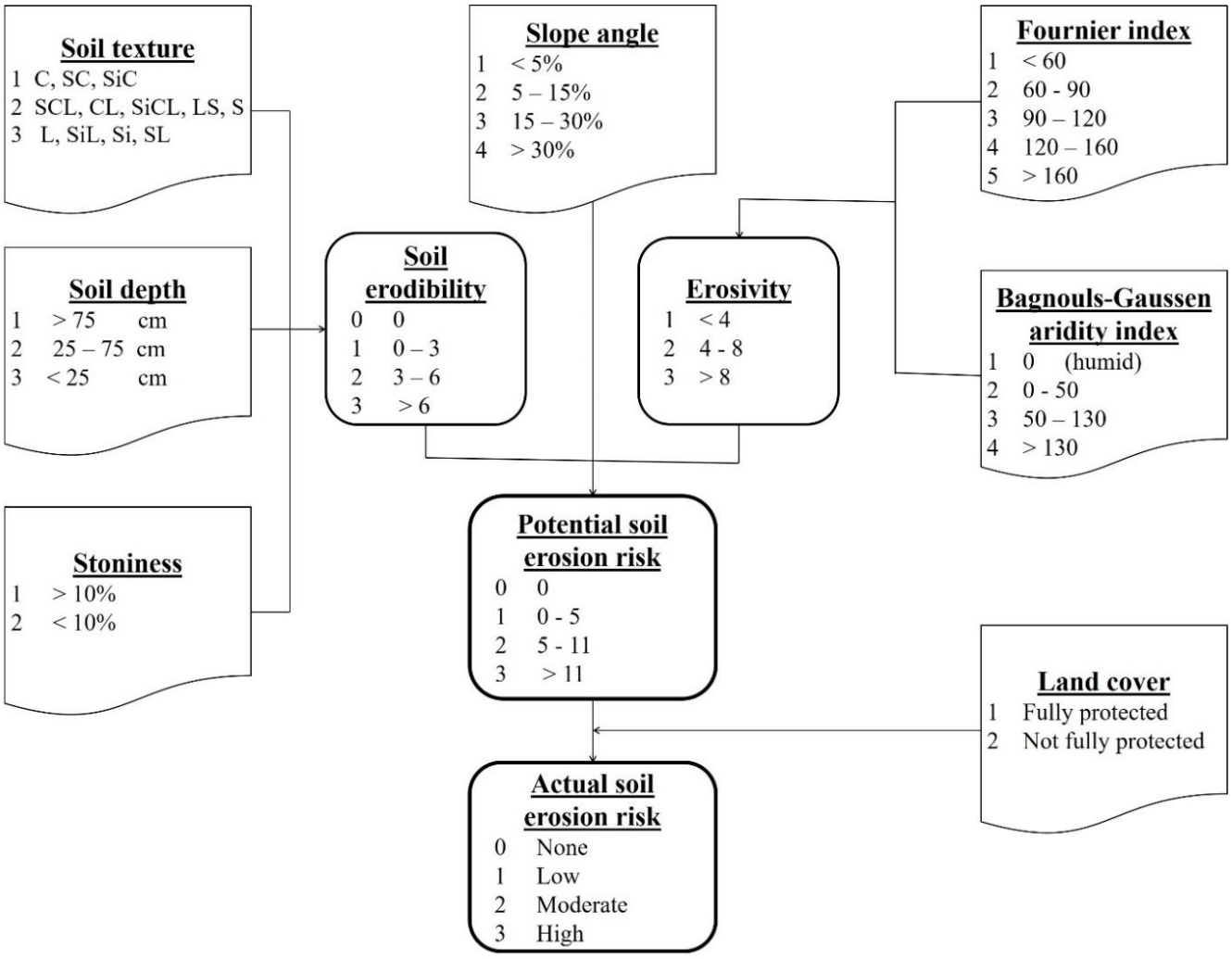

Fig. 5 : Flow diagram of the CORINE Model for erosion assessment (CORINE, 1992).

Table 2 : Meteorological data Matrouh metrological station (2000 – 2018).

Month	Jan.	Feb.	March	April	May	June	July	Aug.	Sep.	Oct.	Nov.	Dec.	Mean
Temperature °C	16.09	14.99	16.95	19.30	21.96	24.72	26.41	26.62	25.31	22.11	18.24	16.54	20.48
Precipitation (mm)	32.05	14.25	9.52	8.41	5.77	0.07	0.00	0.00	3.73	10.16	31.57	32.82	148.35

(Yuksel *et al.*, 2008).

Where, t_i : Average monthly temperature (degrees Celsius).

k_i : calculated when 2ti-pi> 0, (ki) is the proportion of the month if 2ti-pi > 0.

FI and BGI indices are classified as shown in Table 3.

Slope index

It was derived from the DEM using Arc-GIS 10.3 and classified as shown in table 4.

Potential Soil Erosion Risk (PSER) : Soil erodibility and slope maps were combined and then multiplied by erosivity index using spatial analyst extension (Map algebra) of Arc-GIS 10.3 to calculate the PSER as follows:

PSER index = Erodibility index × Erosivity index × Slope index.

Land Cover index : Remote sensing data with GIS techniques can provide beneficial support in extracting the different land cover classes (Yousif and Ahmed, 2019). Therefore, land cover was created using ENVI 5.2 by maximum likelihood supervised classification process on Landsat 8 image (P179/R038 dated in 2019). According to CORINE model, land cover index was classified into two classes: (1) fully protected, which includes forests, bodies of water, construction, roads and rocky Land. (2) Not fully protected which includes land crops and fruit

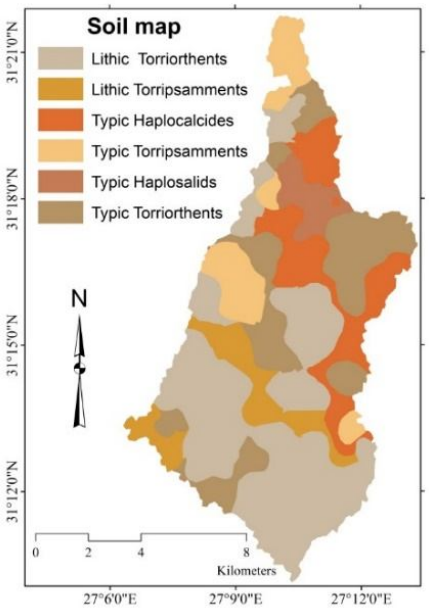

Fig. 6 : Soil taxonomy map of the studied area.

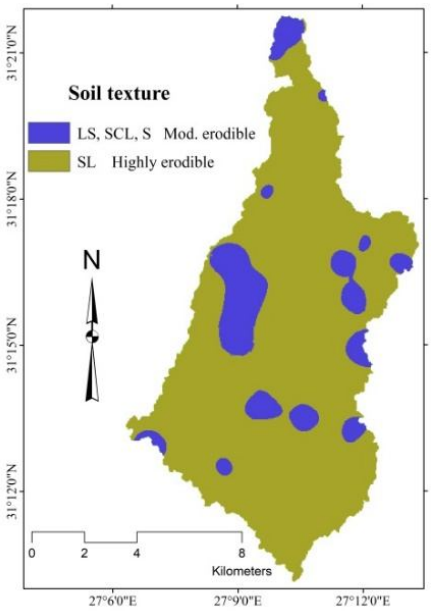

Fig. 7 : Soil texture map the studied area.

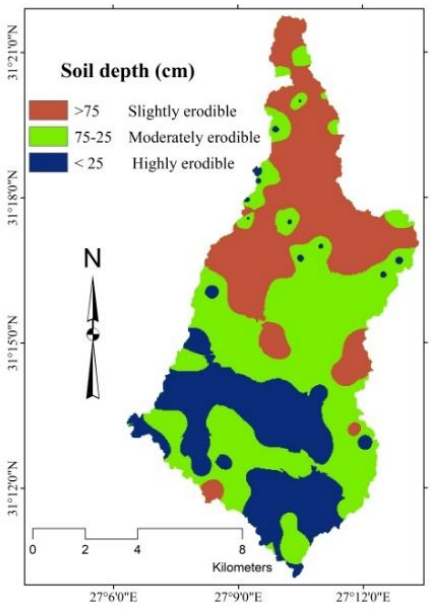

Fig. 8 : Soil depth map the studied area.

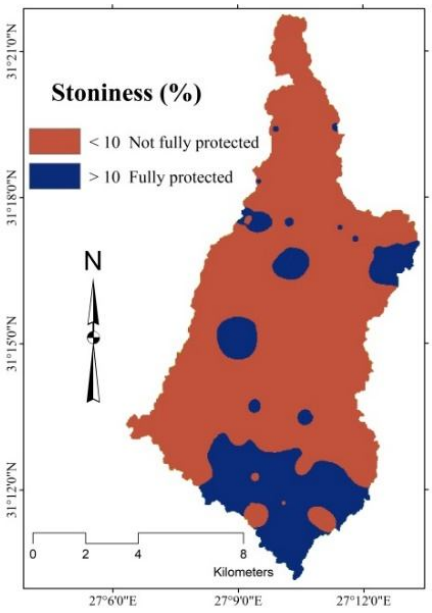

Fig. 9 : Stoniness coverage mao of the studied area.

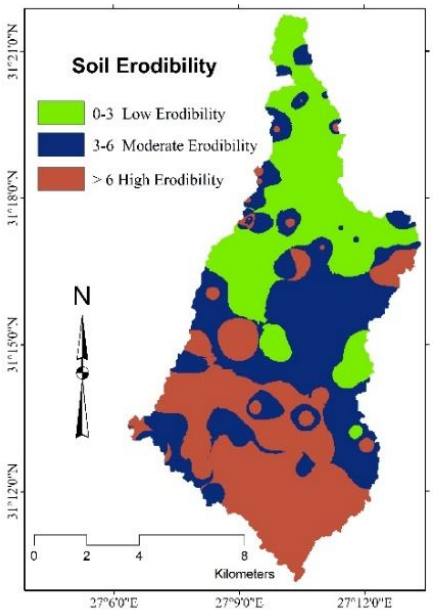

Fig. 10 : Erodibility map of the investigated area.

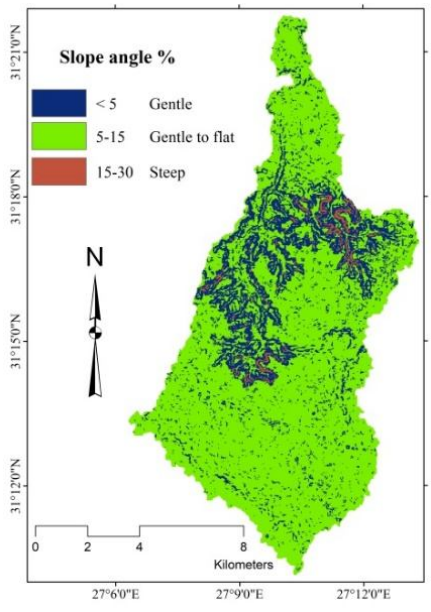

Fig. 11 : The slope map of the investigated area.

trees.

Actual Soil Erosion Risk : Land cover and PSER maps were combined using Spatial Analyst extension (Map algebra) of Arc-GIS 10.3 to generate the ASER as follows:

Index of ASER = PSER index × Land cover index.

Finally, ASER and PSER maps were classified as shown in table 5.

Results and Discussion

Results in table 6 illustrated that, the gravels content ranged from 0 to 44.15%. The common soil texture classes are sandy loam and loamy sand. Soil depth is ranged from shallow to deep soils (15 – 150 cm). Soil pH values varied between 7.11 and 8.76. Soil electrical conductivity is varied from 0.39 to 38.66 dS/m. Calcium carbonate content is ranged between 17.45 and 76.12%. Exchangeable sodium percent varied from 9.47 to 28.21%. Organic matter content is very poor and ranged from to 0.13 to 1.19%.

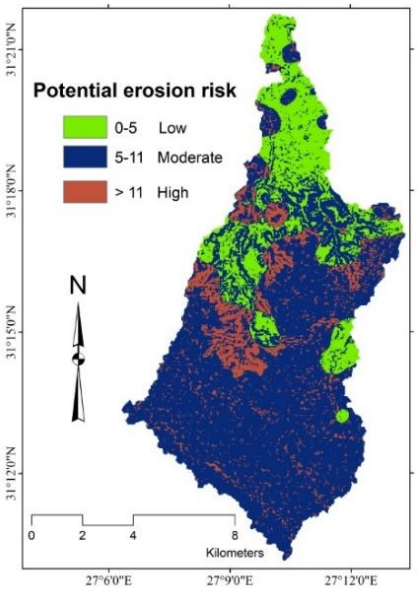

Fig. 12 : Potential erosion risk map of the studied area.

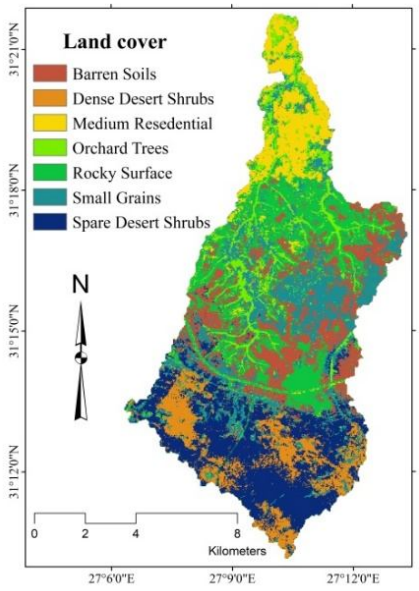

Fig. 13 : Land cover map of the studied area.

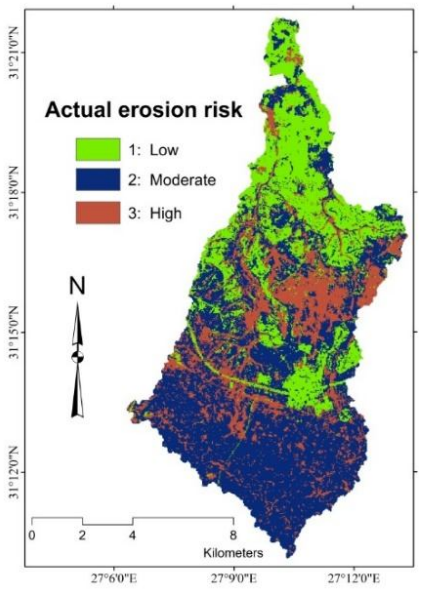

Fig. 14 : Actual soil erosion risk map of the studied area.

Table 3 : Ranking of FI and BGI indices (Aydin and Tecimen, 2010).

Class	FI		BGI		Erosivity	
	Range	Class	Range	Class	Range	Class
1	< 60	Very low	0	Humid	<4	Low
2	60-90	Low	0-50	Moist	4-8	Mode-rate
3	90-120	Mode-rate	50-130	Dry	>8	High
4	120-160	High	>130	Very		
5	>160	Very High		Dry		

Table 4 : Classes of Slope degree by CORINE model.

Class	Classification	Slope Angle (%)
1	Gentle to flat	< 5
2	Gentle	5-15
3	Steep	15-30
4	Very steep	>30

The investigated soils were classified into five sub great groups (Soil Survey Stuff, 2014) as shown in table 7 and fig. 6. The most common sub great group is Lithic Torriorthents with 42.21%, which located in the northern part while the lowest sub great groups is Typic Haplosalids with 4.21%, which located in the southern part.

Soil Erodibility index

Results in table 8 explained that sandy loam was the common soil texture class with 86.54% of the soils, which is characterized as highly erodible soils and low resistant to erosion. While, 13.46% of the soils were Loamy sand, Sand and Sandy clay loam and characterized as moderately erodible soils and moderate resistant to erosion according to CORINE model.

Soil depth is a very important factor in soil erodibility due to the water storage ability of soil profile increased with increasing soil depth (Yuksel *et al*., 2008). Results in Table 8 and Figure 8 illustrated that 24.72% of the soils with a depth of less than 25 cm and characterized as severe tendency for erosion which located in the northern part. About 43.85% of the studied soils with a depth of 25-75 cm and recognized as medium susceptibility for erosion and located mainly in the middle part, while 31.43% of the soils with a depth of more than 75 cm were classified as low tendency for soil erosion which located in the southern part of the basin.

Results in fig. 9 and table 8 showed that 21.58% of the studied soils were characterized as fully protected surface with gravel coverage greater than 10% and located in the southern part, while 78.42% of soils were categorized as not fully protected with coverage less than 10%.

Soil erodibility map was created by overlaying soil texture, depth, and stoniness maps (fig. 10). The erodibility map indicated that 29.02% of the watershed is covered by low erodible soil and located in the southern part of the watershed since the area is highly dominated by deep soils (fig. 10), while 36.55% covered by moderately erodible soil which located in the middle part of the

Table 5 : Classes and ranking of PSER, ASER and land cover (Aydin and Tecimen, 2010).

PSER		**Non**	**Low**	**Moderate**	**High**
		0	**1**	**2**	**3**
		ASER			
Land cover index	(1) Fully protected (FP)	0	1	1	2
	(2) Not fully protected (NFP)	0	1	2	3

Table 6 : Some physical and chemical soil analysis.

P. No.	**Depth (cm)**	**Gravel %**	**Particle size distribution %**				**$CaCO_3$%**	**pH**	**ECdS/m**	**ESP**	**OM%**
			Sand	**Silt**	**Clay**	**Class**					
1	150	6.45	69.83	12.67	17.5	SL	22.46	7.74	9.91	14.21	0.51
2	150	11.38	69.33	11.92	18.75	SL	24.41	7.83	4.57	11.61	1.19
3	90	9.39	74.75	11.25	14	SL	22.15	8.34	1.45	10.09	0.41
4	140	11.03	72.13	9.91	17.96	SL	26.39	8.09	10.05	14.28	0.91
5	100	3.13	81.26	5.38	13.37	SL	18.94	7.41	0.48	9.47	0.23
6	100	4.21	66.43	19.91	13.66	SL	29.14	7.95	20.81	19.52	0.20
7	130	1.50	60.75	25.67	13.58	SL	26.64	7.75	38.66	28.21	0.24
8	120	1.53	79.05	7.92	13.04	SL	33.74	8.42	0.79	9.62	0.43
9	100	0.93	81.88	5.00	13.12	SL	23.06	7.82	0.90	9.67	0.45
10	125	24.03	78.38	8.50	13.12	SL	35.01	7.69	5.84	12.03	0.46
11	120	10.49	75.92	11.88	12.2	SL	37.10	8.14	1.19	9.81	0.36
12	150	2.42	76.55	10.00	13.45	SL	40.02	7.95	0.77	9.61	0.40
13	120	0.00	74.14	15.64	10.23	SL	63.06	7.77	22.75	20.47	0.26
14	130	15.26	69.35	19.09	11.55	SL	25.15	7.99	1.64	10.18	0.25
15	20	11.11	64.68	26.07	9.25	SL	28.00	7.86	3.42	11.05	0.25
16	40	6.07	71.13	9.38	19.5	SL	30.82	7.63	10.43	14.22	0.38
17	150	2.42	76.55	10.00	13.45	SL	40.02	7.95	0.77	9.61	0.40
18	150	0.00	85.18	8.46	6.37	LS	67.07	8.09	10.03	14.27	0.20
19	90	0.00	86.09	10.52	3.4	LS	32.26	8.50	0.80	9.77	0.20
20	20	0.00	73.98	14.15	11.87	SL	28.31	8.76	2.05	10.38	0.28
21	60	0.00	79.85	14.01	6.14	LS	59.27	7.61	10.65	14.57	0.25
22	120	0.00	68.32	20.41	11.27	SL	22.45	7.48	2.07	10.39	0.26
23	130	0.00	68.44	19.49	12.06	SL	33.77	7.57	24.10	21.12	0.24
24	15	0.00	64.95	21.29	13.76	SL	29.58	8.38	0.74	9.74	0.20
25	15	12.87	84.88	5.00	10.12	LS	28.46	7.71	0.58	9.52	0.47
26	15	12.87	84.88	5.00	10.12	LS	28.46	7.71	0.58	9.52	0.47
27	25	41.02	79.88	5.00	15.12	SL	30.31	8.29	0.88	9.66	0.25
28	25	41.02	79.88	5.00	15.12	SL	30.31	8.29	0.88	9.66	0.25
29	30	44.15	74.88	7.50	17.62	SL	34.60	7.99	0.66	9.55	0.29
30	30	44.15	74.88	7.50	17.62	SL	34.60	7.99	0.66	9.55	0.29
31	30	33.45	77.38	5.00	17.62	SL	34.12	7.41	0.88	9.66	0.21
32	30	33.45	77.38	5.00	17.62	SL	34.12	7.41	0.88	9.66	0.21
33	15	9.51	82.38	2.50	15.12	SL	34.39	7.65	0.65	9.55	0.19
34	15	9.51	82.38	2.50	15.12	SL	34.39	7.65	0.65	9.55	0.19
35	25	4.92	77.38	5.00	17.62	SL	29.12	7.11	2.57	10.47	0.22
36	100	2.42	83.26	5.38	11.37	LS	17.45	7.27	0.39	9.42	0.16
37	20	9.10	68.73	23.62	7.65	SL	25.90	7.90	1.07	9.90	0.25

Table 6 continued...

Table 6 continued...

38	16	25.16	74.88	5.00	20.12	SCL	32.41	7.86	0.90	9.67	0.37
39	150	2.28	84.88	6.67	8.45	LS	23.78	7.77	0.63	9.54	0.22
40	120	4.24	92.38	2.50	5.12	S	14.78	7.67	0.69	9.57	0.13
41	40	8.67	74.88	12.50	12.62	SL	26.77	7.38	10.73	14.37	0.79
42	40	8.67	74.88	12.50	12.62	SL	26.77	7.38	10.73	14.37	0.79
43	25	6.90	77.38	7.50	15.12	SL	26.47	8.26	2.29	10.33	0.59
44	50	29.01	86.63	2.50	10.87	LS	18.12	8.11	0.54	9.50	0.34
45	25	6.17	82.38	5.00	12.62	SL	21.22	7.79	0.66	9.55	0.20
46	25	5.58	84.88	2.50	12.62	LS	22.83	7.69	0.68	9.56	0.70
47	65	11.87	69.69	11.35	18.97	SL	28.82	7.76	0.61	9.53	0.40
48	45	9.02	79.05	6.67	14.29	SL	24.41	7.77	0.67	9.56	0.56
49	8	0.00	63.42	23.36	13.22	SL	22.61	8.69	0.52	9.63	0.25
50	20	16.85	72.38	12.50	15.12	SL	38.26	7.86	0.58	9.52	0.28
51	15	8.52	79.88	7.50	12.62	SL	29.03	8.26	0.73	9.59	0.35
52	65	6.26	79.69	5.19	15.12	SL	26.51	7.74	0.74	9.59	0.32
53	16	25.16	74.88	5.00	20.12	SCL	32.41	7.86	0.90	9.67	0.37
54	50	3.92	77.38	10.00	12.62	SL	76.12	7.90	10.50	14.26	0.64

SL, sandy loam; LS, loamy sand; SCL, sandy clay loam; S, sand.

Table 7 : Soil taxonomy of the investigated soils.

Soil taxonomy	Area (km^2)	Area (fed)	%
Lithic Torriorthents	45.16	10751.89	42.21
Lithic Torripsamments	9.19	2188.55	8.59
Typic Haplocalcides	15.58	3709.96	14.56
Typic Haplosalids	4.50	1071.30	4.21
Typic Torriorthents	21.98	5232.45	20.54
Typic Torripsamments	10.58	2519.64	9.89
	106.99	25473.79	100

and classified as low rainfall erosion index.

Slope map

It has an effective influence on controlling erosion rates due to its significant impact on surface runoff and the water infiltration in the soil (Dragut and Eisank, 2012). It was created from the DEM and classified based on the CORINE model (fig. 11). The results illustrated that 77.77% of the investigated area has less than 5% slope (table 9). While 20.81% has gentle slope (5-15%) and the remnant area (1.42%) has a steep slope (15-30%).

Table 8 : Distribution of soil texture, depth, stoniness and erodibility of the studied area.

Texture			Soil depth			Stoniness			Erodibility		
Class	Area (km^2)	%	Class	Area (km^2)	%	Class	Area (km^2)	%	Class	Area (km^2)	%
	14.40	13.46	1 >75	33.63	31.43				0-3 Low	31.04	29.02
2 LS – S – SCL			2 75 - 25	46.91	43.85	1 >10	23.09	21.58	3-6 Moderate	39.10	36.55
3 SL	92.58	86.54	3 <25	26.45	24.72	2 <10	83.90	78.42	>6 High	36.84	34.43
Total	106.99	100		106.99	100		106.99	100	106.99	106.99	100

watershed. The rest of the area (34.43%) in the northern part is covered by highly erodible soil due to its shallow soils (table 8).

Erosivity index (EI)

It was calculated using meteorological data obtained from the Matrouh metrological station (table 2). Results indicated that FI value was 24.37 and classified as a very low. While the BGI was 123.17 and classified as dry according to CORINE. Finally, the EI value is equal to 3

Potential Soil Erosion Risk

PSER map was generated by overlaying soil erodibility, erosivity and slope maps (fig. 12). Results indicated that 69.78% of the area classified as moderate PSER which located in the north and middle part of the watershed. Low PSER covers 8.52% of the area and located in the southern part of the studied area. While 11.70 % of the area were categorized as high PSER which located in the middle of the watershed (table 9).

Table 9 : Spatial distribution of slope, land cover, PSER and ASER of studied area.

Slope				Land cover				PSER				ASER			
Class		Area (km^2)	%	Class		Area (km^2)	%	Class		Area (km^2)	%	Class		Area (km^2)	%
1	<5	83.20	77.77	1	FP	30.63	28.63	1	Low	19.80	18.52	1	Low	29.69	27.75
2	5-15	22.27	20.81	2	NFP	76.36	71.37	2	Moderate	74.59	69.78	2	Moderate	53.89	50.37
3	15-30	1.52	1.42		-	-	-	3	High	12.51	11.70	3	High	23.41	21.88
Total		106.99	100			106.99	100			106.99	100			106.99	100

Land Cover Index

It plays a main role in decreasing the runoff and reducing the severity of erosion, due to protecting the soil surface (Estoquea and Murayama, 2011). Land cover map (fig. 13) showed that 28.63% of the area was classified as a fully protected areas, which include residential and rocky areas (table 9). The rest area represented 71.37% and classified as not fully protected which include barren soils, spare and dense Shrubs, orchard trees and small grains.

Actual Soil Erosion Risk

The ASER map illustrated the variance between the areas of PSER and ASER due to the effect of land cover in the hazard of erosion (fig. 14). Results indicated that 50.37% of soils was classified as moderately ASER, which located in the north and middle part of the watershed (table 9). While 27.75% and 21.88% were classified as low and high ASER, respectively. Areas with ASER located in the middle and north part, while areas with high ASER located mainly in the southern part of the area. The areas categorized as low PSER were increased from 18.52% to 27.75% in the ASER, after combining the land cover map due to the improper agricultural activities. On the other hand, the total areas classified as high and moderate PSER were decreased from 81.48% to 72.25% in the ASER, due to the effect of land cover on decreasing risk of soil erosion.

Conclusion

This research work was amid at using the methodology of CORINE model within GIS environment to assess the spatial heterogeneity of soil erosion risk in Wadi El-Raml watershed, north western coast of Egypt. The PSER map explained that small area of the watershed (11.70%) had high risk and a large area (69.78%) had moderate PSER. On the other hand, the ASER map indicated that a small area of the watershed (21.88%) had high risk and a large area (50.37%) had moderate ASER. However, the medium and high erosion risk was decreased from 81.48% to 72.25% in the ASER map. The most common factors that resulted in high erosion risk included soil texture, land cover and soil depth. Therefore, suitable agriculture land use activities should be carried out to minimize soil erosion. This work indicated that the CORINE model integrated with GIS and RS has very effective and accurate potential for soil erosion risk assessment.

References

Aahikari, R. N., S. Chittaranjan, M. S. Rama Mohan Rao and V. Husenappa (2004). Hydrological data analysis for small black soil agricultural catchments in dryland zone of karnataka. *Indian J. Agric. Res.*, **38 (3)**: 196 - 201.

Aksoy, H. and M. L. Kavvas (2005). A review of hillslope and watershed scale erosion and sediment transport models. *Catena*, **64 (2-3)**: 247–271.

Aydýn, A. and H. S. Tecimen (2010). Temporal soil erosion risk evaluation: a CORINE methodology application at Elmalý dam watershed, Istanbul. *Environ Earth Sci.*, **61** : 1457–1465.

Cilek, A., S. Berberoglu, M. Kirkby, B. Irvine, C. Donmez and M. A. Erdogan (2015). Erosion modelling in a Mediterranean subcatchment under climate change scenarios using Pan-European Soil Erosion Risk Assessment (PESERA). *ISPRS - Int. Archives of the Photogrammetry, Remote Sensing and Spatial Information Sciences* **XL–7/W3**: 359–365.

CORINE (1992). CORINE: soil erosion risk and important land resources in the Southeastern regions of the European community. EUR 13233, Luxembourg, Belgium, pp 32–48

De Vente, J., J. Poesen and G. Verstraeten (2005). The application of semi-quantitative methods and reservoir sedimentation rates for the prediction of basin sediment yield in Spain. *Journal of Hydrology*, **305(1-4)** : 63–86.

Dragut, L. and C. Eisank (2012). Automated object-based classification of topography from SRTM data. *Geomorphology*, **141-142**: 21-33.

Edosomwan, N. L., E. Obazuaye and E. Uwa Edosomwan (2013). Impacts of dam on characteristics of tropical rainforest soils and sediments in south central Nigeria. *Indian J. Agric. Res.*, **47(1)** : 73-77.

Egyptian Meteorological Authority (2018). *Climatic Atlas of*

Egypt. Ministry of Transport, Cairo, Egypt.

El-Nady, M. A. and M. M. Shoman (2017). Assessment of Soil Erosion Risk in The Basin of Wadi Maged in Northern West Coast of Egypt Using CORINE Model and GIS Techniques. *Egypt. J. Soil Sci*., **57 (1)**: 31 – 45.

El-Shazely, E. M., M. A. Abdel Hady and M. A. El-Ghawaby (1975). Geologic interpretation of LANDSAT satellite images for west Nile Delta area, Remote sensing research project. Academic of scientific research and technology, Cairo, Egypt.

Eroglu, H., G. Cakir, F. Sivrikaya and A. E. Akay (2010). Using high resolution images and elevation data in classifying erosion risks of bare soil areas in the Hatila Valley Natural Protected Area, Turkey. *Stoch Environ Res Risk Assess*, **24** : 699–704.

ESRI (2012). *Environmental Systems Research Institute* (ESRI) Press. Redlands, California.

Estoquea, R. C. and Y. Murayama (2011). Spatio-Temporal Urban Land Use/Cover Change Analysis in a Hill Station: The Case of Baguio City, Philippines. *Procedia Social and Behavioral Sciences*, **21** : 326–335.

Husnjak, S., I. Simunic and I. Tursic (2008). Soil erosion risk in Croatia. *Cereal Res Commun.*, **36** : 939–942.

Ýmamoglu, A., Y. D. Turan, O. Dengiz and F. Saygin (2014). Soil erosion risk evaluation: Application of Corine Methodology at Engiz Watershed, Samsun. *Current Advances in Environmental Science*, **2(1)** : 15–21.

Jakhar, P., D. Barman, H. C. Home Gowda and M. Madhu (2012). Multitier cropping system for profitable resource conservation and sustainable management of sloping lands of eastern India. *Indian J. Agric. Res*., **46 (4)**: 309 – 316.

Lakkad, A. P., G. R. Patel, K. N. Sondarva and P. K. Shrivastava (2018). Estimation of sediment delivery ratio at sub-watershed level using revised and modified USLE. *Agric. Sci. Digest*., **38 (1)**: 11-16.

Omuto, C. T. and R. R. Vargas (2009). Combining pedometrics, remote sensing and field observations for assessing soil loss in challenging drylands: a case study of northwestern Somalia. *Land Degrad Dev*., **20** : 101–115

Shpkinah, E. D. and R. Saraswathy (2005). Impacts of soil erosion by water - a review. *Aqric Rev.*, **26 (3)**: 195·202.

Singh, A. K., M. Kothari, P. K. Mishra, V. Kumar, G. V. Srinivasa Reddy and R. C. Purohit (2007). Soil erosion research under simulated conditions for Black soils of southern India - a review. *Agric. Rev.*, **28(1)** : 63-68.

Soil Survey Staff (2014). *Key to Soil Taxonomy*. Twelfth Edition, U.S.D.A., Washington, D.C., 372 p.

USDA (2014). Kellogg Soil Survey Laboratory Methods Manual. United States Department of Agriculture. *Soil Survey Investigation Report No. 42* Version 5.0, 1031p.

Yousif, I. A. H. and A. S. Ahmed (2019). Integration of Land Cover Changes and Land Capability of Wadi El-Natrun Depression Using Vegetation Indices. *Egypt. J. Soil. Sci*., **59(4)** : 385-402.

Yuksel, A., R. Gundogan and A. E. Akay (2008). Using the remote sensing and GIS technology for erosion risk mapping of Kartalkaya Dam Watershed in Kahramanmaras, Turkey. *Sensors*, **8** :4851–4865.